Molecular and Cellular Biochemistry (2019) 456:191–204
https://doi.org/10.1007/s11010-019-03504-z

Attenuation of calmodulin regulation evokes Ca^{2+} oscillations: evidence for the involvement of intracellular arachidonate-activated channels and connexons

Egor A. Turovsky[1] · Valery P. Zinchenko[1] · Nikolai P. Kaimachnikov[1]

Received: 16 August 2018 / Accepted: 1 February 2019 / Published online: 11 February 2019

Abstract
Intracellular Ca^{2+} controls its own level by regulation of Ca^{2+} transport across the plasma and organellar membranes, often acting via calmodulin (CaM). Drugs antagonizing CaM action induce an increase in cytosolic Ca^{2+} concentration in different cells. We have found persistent Ca^{2+} oscillations in cultured white adipocytes in response to calmidazolium (CMZ). They appeared at [CMZ] > 1 μM as repetitive sharp spikes mainly superimposed on a transient or elevated baseline. Similar oscillations were observed when we used trifluoperazine. Oscillations evoked by 5 μM CMZ resulted from the release of stored Ca^{2+} and were supported by Ca^{2+} entry. Inhibition of store-operated channels by YM-58483 or 2-APB did not change the responses. Phospholipase A_2 inhibited by $AACOCF_3$ was responsible for initial Ca^{2+} mobilization, but not for subsequent oscillations, whereas inhibition of $iPLA_2$ by BEL had no effect. Phospholipase C was partially involved in both stages as revealed with U73122. Intracellular Ca^{2+} stores engaged by CMZ were entirely dependent on thapsigargin. The oscillations existed in the presence of inhibitors of ryanodine or inositol 1,4,5-trisphosphate receptors, or antagonists of Ca^{2+} transport by lysosome-like acidic stores. Carbenoxolone or octanol, blockers of hemichannels (connexons), when applied for two hours, prevented oscillations but did not affect the initial Ca^{2+} release. Incubation with La^{3+} for 2 or 24 h inhibited all responses to CMZ, retaining the thapsigargin-induced Ca^{2+} rise. These results suggest that Ca^{2+}-CaM regulation suppresses La^{3+}-sensitive channels in non-acidic organelles, of which arachidonate-activated channels initiate Ca^{2+} oscillations, and connexons are intimately implicated in their generation mechanism.

Keywords Ca^{2+} oscillations · Calmodulin · Arachidonic acid · Connexons · Calmidazolium · Adipocytes

Introduction

Intracellular Ca^{2+} is a key messenger for various external signals that act on cell receptors and control a multitude of cell functions. The level of cytosolic Ca^{2+} at rest and under stimulation is governed by autoregulatory effects on its channels, pumps and exchangers in the plasma membrane (PM) and membranes of intracellular organelles serving as Ca^{2+} stores. In particular, direct Ca^{2+} binding to the subunits of inositol 1,4,5-trisphosphate receptor (IP_3R) and ryanodine receptor (RyR) of the endoplasmic reticulum (ER) opens these channels and causes calcium-induced calcium release (CICR) from the organelle filled by sarco/endoplasmic reticulum Ca^{2+}-ATPase (SERCA). Many of Ca^{2+} effects are mediated by ubiquitous protein calmodulin (CaM), which changes its conformation upon Ca^{2+} binding and activates or inhibits the targets including the Ca^{2+}channels and PM Ca^{2+}-ATPase (PMCA). Such modulation by CaM can be indirect, proceeding through the CaM-dependent kinase or phosphatase, as well as through a range of intermediary effectors. Dysregulation of Ca^{2+} signaling is involved in cell death, altered proliferation and major diseases [1–3]. This complex Ca^{2+} signaling system typically responds to stimuli by oscillations. They are further decoded through CaM or other Ca^{2+} sensors that selectively activate various cellular processes, depending on both the frequency and the amplitude of the repetitive events. It is generally accepted that the mechanism of Ca^{2+} oscillations is based on CICR [1, 4].

Calcium entry through PM necessary for persistent, long-lasting Ca^{2+} elevations and oscillations can be provided

✉ Nikolai P. Kaimachnikov
nkai@mail.ru

[1] Institute of Cell Biophysics of the Russian Academy of Sciences, Pushchino, Moscow Region, Russia 142290

by different channels, among which store-operated Ca^{2+} (SOC) channels are widespread. Selective calcium release-activated-calcium (CRAC) channels of this type are formed by Orai1 proteins. Cationic TRPC channels mediate SOC entry (SOCE) and store-independent entry (non-SOCE) [5]. Under low agonist concentrations that cause oscillations, Ca^{2+} entry may be determined by store-independent, arachidonate-regulated Ca^{2+} (ARC) channels of PM, which are also activated by leukotriene C_4 [5, 6]. ARC channels are heteromultimers of Orai1 and Orai3 subunits compared to homohexameric CRAC channels [5]. Connexin (Cx) hemichannels (connexons) were shown to be important for oscillations in some cells [7–9]. These hemichannels form intercellular gap junctions, while in an unopposed state they function as channels for ions and small molecules such as ATP and NAD^+, and the released substances may activate cell receptors [10]. Connexons are also present in cytoplasmic structures, which perform their biosynthesis and degradation and communicate with PM by trafficking [10, 11]. It was suggested that vesicle-bound connexons might mediate NAD^+ transport between subcellular compartments [12], but in general, the Ca^{2+}-signaling role of intracellular connexons remains obscure. Pannexin proteins form channels (not gap junctions) that resemble connexons [10, 13]. Different PM components of Ca^{2+} transport can be transferred into the cell by endocytosis forming endosomes that are gradually acidified by the vacuolar-type H+-ATPase (V-ATPase) and eventually fuse with lysosomes. The proton gradient is used for accumulation of Ca^{2+}, released thereafter by NAADP activating two-pore channels. The acidic stores can participate in CICR and formation of Ca^{2+} signals [14].

Despite numerous data on CaM effects exerted on the participants of Ca^{2+} signaling, the total impact of CaM on Ca^{2+} dynamics, and especially its role in oscillations are not fully understood. Application of different CaM antagonists increased cytosolic Ca^{2+} via stimulation of release and entry [15–22], suggesting the repressive Ca^{2+}-CaM influence on the Ca^{2+} level at the resting state. The same approach indicated modulation by CaM of agonist-induced Ca^{2+} oscillations in hepatocytes [23] and megakaryocyte [24]. We had observed that calmidazolium (CMZ) itself induced prolonged Ca^{2+} oscillations in white adipocytes [25]. The imidazole derivative CMZ, or R24571, belongs to the compounds whose binding to the hydrophobic surfaces of CaM prevents the interaction of CaM with the target proteins [26]. Adipocytes are prone to Ca^{2+} oscillations evoked by a number of agonists acting through IP_3R-dependent or RyR-dependent signaling pathways [25, 27, 28]. Apart from ER, these cells have endocytic structures and specialized vesicles providing recycling and storage of the glucose transporter GLUT4 [29]. Non-ER Ca^{2+} stores might be involved in the signaling network, since addition of exogenous NAADP to adipocytes resulted in Ca^{2+} transients [30].

The aim of the present study was to characterize the impact of CaM antagonists, attenuating CaM-mediated regulation, on cytosolic Ca^{2+} in adipocytes and to reveal the underlying mechanism with the use of inhibitors of potentially involved processes. We investigated whether this mechanism is based on IP_3R- or RyR-mediated Ca^{2+} release and tested the participation of other pathways able to mobilize Ca^{2+}. The obtained data indicate stimulation of arachidonic acid (AA) production and Ca^{2+} release through AA-activated (probably, ARC) channels, with oscillations being driven by connexons. It is proposed that these channels, typical for PM, may be functional, at least under certain conditions, in organelles related to PM by trafficking, and the organellar connexons could generate oscillations due to their own CICR.

Materials and methods

Isolation of preadipocytes

All animal studies were approved by the Animal Ethic Committee of the Institute of Cell Biophysics, Russian Academy of Sciences, and are in accordance with the European Communities Council Directive (86/609/EEC). NMRI mice (aged 3–5 weeks) were decapitated after a brief (45–60 s) anesthesia with carbon dioxide before sacrifice. Mice were subjected to cervical dislocation and disinfected with 70% ethanol prior to dissection. All operations were performed in a sterile environment on ice. White adipose tissue was removed from the epididymal fat depot and placed in a Petri dish with cold DMEM-medium (Sigma, USA). Scissor-minced white adipose tissue was transferred into a tube containing sterile DMEM with 7 mg type II collagenase (Sigma-Aldrich, USA) and 4% bovine serum albumin (BSA, free from fatty acids, Sigma, USA). Then, the tissue was incubated for 18 min at 37 °C. To stop the collagenase enzymatic reaction, the tube was chilled on ice for 20 min with intermittent shaking followed by filtration through 250 µm filter and centrifugation at 1000 g for 10 min. The pellet was then resuspended in cold DMEM medium, filtered through 50 µm filters and centrifuged at 1000 g for 10 min. Finally, the pellet was resuspended in cultural medium containing: DMEM, 10% fetal bovine serum (FBS, Gibco, USA), 4 mM L-glutamine (Sigma, USA), 4 nM insulin (NovoNordisk, Denmark), 0.004% gentamicin and 25 µg/ml sodium ascorbate (Sigma, USA). The obtained suspension contained preadipocytes, since mature adipocytes carry vesicles of fat and do not precipitate under the given conditions.

Cultures of white adipocytes

100 µl droplets of culture medium containing 3×10^4 preadipocytes were placed on round coverglasses (25 mm in diameter), which were then transferred into 35 mm Petri dishes. 6 h after adhesion of the cells to the glass, additional culture medium was added to the Petri dishes. On the third day, the medium in the dishes was replaced with a fresh portion of medium, which included 10 nM of cytosine arabinoside (Sigma, USA) to suppress proliferation of fibroblasts, and incubation in CO_2 atmosphere was continued for 8 h. After that the medium was replaced with fresh culture medium. On the ninth day of cultivation in the CO_2 incubator at 37 °C, the cells formed a monolayer and became differentiated.

Measurements of cytosolic calcium concentration

Measurements of cytosolic [Ca^{2+}] were performed by fluorescent microscopy using fura-2/AM (Invitrogen, USA), a ratiometric fluorescent calcium indicator. Cells were loaded with the probe dissolved in Hanks balanced salt solution (HBSS), containing 10 mM HEPES (both from Gibco, USA), pH 7.4, at the final concentration of 5 µM at 37 °C for 40 min with subsequent 15 min washout. The coverslip containing the cells loaded with fura-2 was then mounted in the experimental chamber. During the experiment we used a perfusion system, which enables complete replacement of the cell bathing solution within 30 s. Calcium-free medium contained 0.5 mM EGTA. Axiovert 200M based imaging system (Carl Zeiss, Germany) equipped with a HBO100 mercury lamp, an AxioCam HSm CCD camera and a MAC5000 high-speed excitation filter wheel was used. Fura-2 fluorescence was excited at two wavelengths using band-pass filters BP 340/30 and BP 387/15; fluorescence was registered in the wavelength range of 465–555 nm. The excitation light intensity was lowered using 25 and 5% neutral density filters to prevent phototoxicity. Image frames were acquired at 3 s intervals with a Plan Neofluar 10×/0.3 objective.

Assessment of cell viability

The amount of viable and dead cells was estimated using staining with 1 µg/ml propidium iodide (PI, Invitrogen, USA). PI has red fluorescence and penetrates only into necrotic cells with damaged outer membranes and can also indicate abnormally opened Cx hemichannels. Cells were incubated with PI for 15 min and then washed 3 times with HBSS. To register the PI fluorescence, Filterset 45 (Carl Zeiss, Germany) was used.

Low temperature experiments

Probe loading (40 min) and washout (15 min) were performed at 37 °C. Then the chamber with cells (1 ml of medium) was placed into a refrigerator in an ice-cold container and chilled to 4 °C. Tubes containing reagents for additions and washing media were cooled simultaneously. The cells were loaded with PI on ice and then incubated in a refrigerator for 15 min. Before the experiment, the region of interest was rapidly photographed, and during the subsequent observations (up to 5 min) the temperature was maintained at about 4 °C.

Data analysis

The time lapse image sequences were analyzed using ImageJ 1.44 (NIH Image, Bethesda, MD, USA). Graphs were plotted using the OriginPro 8.0 software (Microcal Software Inc., Northampton, MA, USA). The statistical analysis was performed using the same software. The difference between the two sets of data was considered to be significant at $P < 0.05$ (lower levels are indicated) following the Student's unpaired two-tailed t test. The results are presented as means ± SEM or as a representative calcium signal of the cells, where *n* stands for the number of cells possessing the given pattern of Ca^{2+} behavior. A number of independent experiments are indicated (by default, data from a single experiment). *N* denotes the number of cells analyzed in the given experiment. Fractions of cells displaying any considerable Ca^{2+} responses (RF), oscillations (OF), and a prolonged lag (taken as > 1 min) before the Ca^{2+} rise (LF) were calculated as their corresponding *n*/*N*, then used to determine the mean values. Oscillations were defined as Ca^{2+} changes with 3 or more peaks irrespective of their pattern. Cessation of oscillations was defined as a longer distance between the last peak and the end time compared to the maximum distance between the preceding peaks.

Results

Ca^{2+} responses to CaM antagonists CMZ and TFP

Addition of CMZ to white adipocytes caused dose-dependent changes in the cytosolic Ca^{2+} concentration. Quantitative characteristics of these responses are presented in Fig. 1a. At 1 µM CMZ, no appreciable responses were detected among 90 cells in three independent experiments, and the next concentration of 2.5 µM was half-effective for the response fraction (RF). This implies the existence of a steep threshold between 1 and 2.5 µM CMZ. The responses consisted mainly of oscillations (defined as having not less than three peaks) represented by the oscillation fraction (OF), reaching

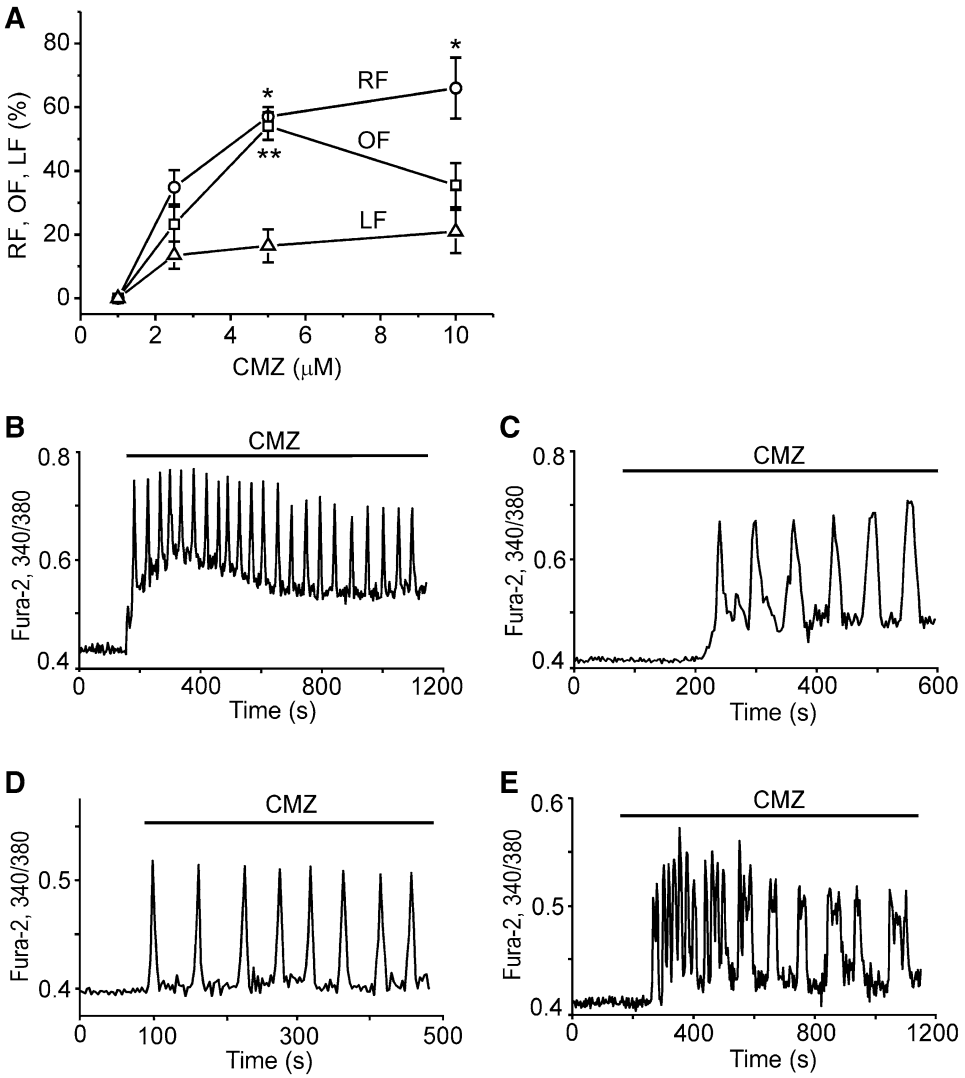

Fig. 1 Dose–response relationship and oscillations of cytosolic Ca^{2+} in single adipocytes at 5 μM CMZ. **a** RF, OF and LF are fractions (relative to *N*) of cells displaying, correspondingly, any responses, oscillations, and time lag > 1 min before a response. Data of 7 (for 5 μM CMZ), 4 (10 μM) or 3 (1 and 2.5 μM) independent experiments with $N \geq 25$ cells incubated for 5.5–16.5 min with CMZ are included. $^{*}P < 0.05$, $^{**}P < 0.01$ vs 2.5 μM CMZ. **b–e** represent same experiments as in (**a**) for 5 μM CMZ, $N = 28–69$, and 361 cells in total. RF = 57.1 ± 3.0%, OF = 54.1 ± 4.3%, LF = 16.5 ± 5.2%, and 7.2 ± 1.5% oscillations stopped. **b** Immediate Ca^{2+} rise followed by oscillations with a gradual decrease in the Ca^{2+} level. **c** Lag phase is present, with no decline in the Ca^{2+} level. **d** Baseline oscillations without the lag. **e** Complex oscillations with a high-frequency component and the initial lag. Mode (**d**) was minor (≤ 17.6% of oscillations, mean 6.2 ± 2.3%), and mode (**e**) occurred occasionally

maximum at 5 μM CMZ. The fraction of the remaining patterns, pulses or transients with 1–2 peaks, when expressed as a percentage to the responded cells, was the lowest (5.4%) at 5 μM CMZ and increased to 46.2% at 10 μM CMZ, thus replacing the oscillatory mode. Responses of all types could have a lag phase before a rapid Ca^{2+} rise. The relative number of responses with lag > 1 min (lag fraction, LF) was rather constant, and the ratio to the responded cells was 29–39%. For the detailed analysis presented below, 5 μM concentration of CMZ was chosen, at which the oscillatory mode was most expressed.

Figure 1b–e shows time courses of responses, mostly possessing the shape of a rapid Ca^{2+} rise with subsequent sustained oscillations on the elevated level that could slowly drift, still staying above the resting state (Fig. 1b, c). Only ≤ 12% of oscillations in each of seven experiments ceased during exposure times up to 16.5 min. The oscillations were mainly represented by sharp spikes with a sub-minute period, ranging from several seconds to a few minutes in some cells. During the baseline oscillations (Fig. 1d), the Ca^{2+} concentration between all spikes resumed the pre-stimulation level. High-frequency oscillations also occurred, which could be imposed upon increases of low frequency in the form of rapid bursts (Fig. 1e). The level of Ca^{2+} during the time lag did no change for some period right after CMZ application, and then an accelerating or abrupt Ca^{2+} elevation took place as shown in Fig. 1c, e. These response patterns suggest that the mechanism of CMZ-induced Ca^{2+} rises can possess specific traits of its manifestation in particular adipocytes. Analogous patterns of drifting oscillations were previously found in the same cell cultures stimulated by acetylcholine and phenylephrine [25, 27].

In view of possible non-specific effects of CMZ not mediated by CaM, we also used another antagonist of CaM, trifluoperazine (TFP), belonging to the phenothiazine family [26]. TFP applied in the same concentration range as CMZ, led to robust oscillations (Fig. 2) closely resembling

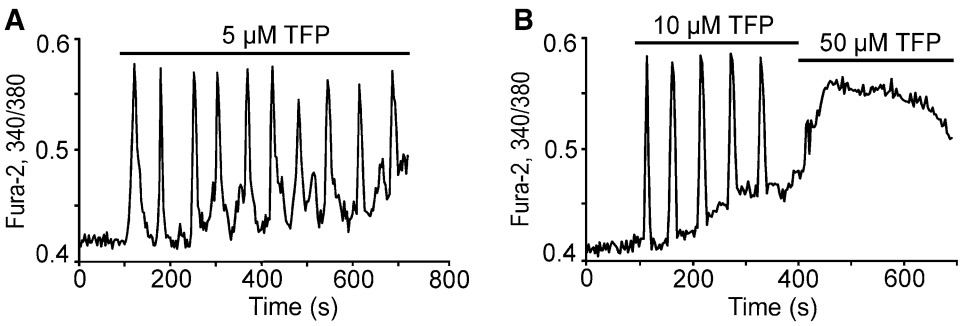

Fig. 2 Ca^{2+} responses to three doses of TFP. **a** Typical oscillations at 5 μM TFP, $n = 23$, RF = 65.8%, $N = 38$. **b** Oscillations at 10 μM TFP ($n = 13$, RF = 53.7%) followed by a transient at 50 μM TFP, $N = 41$

the CMZ-evoked ones in respect to their notched form, amplitude, frequency and duration. At 5 μM TFP (Fig. 2a), oscillations occurred in the vast majority (92%) of responding cells. As a result of higher TFP concentration 10 μM, the oscillatory responses decreased to 59.1%, and subsequent application of 50 μM TFP produced only a transient (Fig. 2b). Taking into account essential similarities between Ca^{2+} responses to CMZ and TFP, we further used CMZ.

Role of Ca^{2+} entry and SOC channels

The medium with normal Ca^{2+} concentration was replaced for nominally Ca^{2+}-free with addition of EGTA as Ca^{2+} chelator to define the role of the total Ca^{2+} entry via calcium-conducting channels of all types. After 30-min preincubation in this medium, cells responded to CMZ with RF, OF and LF indices, not significantly different from those (Fig. 1) in the normal medium. The main pattern was a transient with superimposed oscillations declined close to the initial Ca^{2+} level (Fig. 3a). Most oscillations terminated before the end time in contrast ($P < 0.05$) to persistent oscillations in Fig. 1, where only 7.2% vanished. Subsequent inhibition of the sarco/endoplasmic reticulum Ca^{2+}-ATPase (SERCA) by thapsigargin (TG), that empties the TG-sensitive stores, elicited the response of a similar height as that of CMZ-induced rises (Fig. 3a), not differing from that without CMZ (Fig. 3b) or from that without the preceding Ca^{2+} withdrawal (see the legend to Fig. 7d). This indicates no substantial depletion of the overall TG-sensitive stores during the 30-min absence of Ca^{2+} entry, or during the period of CMZ action. Besides, since CMZ did not lower the rate of Ca^{2+} recovery driven by PMCA (Fig. 3a), its activation by Ca^{2+}-CaM [1] did not account for the increased net Ca^{2+} influx in the normal medium. Thus, oscillations in the CMZ-stimulated adipocytes are produced by the periodic Ca^{2+} release from an intracellular store, whereas Ca^{2+} entry enables sustained high-amplitude oscillations.

The presence of activatable SOC channels in adipocytes [25] together with the lack of store depletion raise the question whether these channels are involved in Ca^{2+} responses to CMZ. It was shown that the SOC channel inhibitor, YM-58483 (also known as BTP2), had a submicromolar half-maximum concentration, with its potency rising by more than an order for hours of preincubation [31]. In our experiments, 1 μM YM-58483 added during CMZ-induced oscillations did not cause a clear-cut immediate effect in respect to the slow component, frequency or amplitude, and oscillations largely persisted (Fig. 3c). Ca^{2+} oscillations were also unaffected by short preincubation with 2-APB (see below), that inhibits [32] the SOC channels. Hence, these PM channels rapidly accessible to the two inhibitors are not indispensable to CMZ-induced oscillations. The possibility of delayed effects was explored by prolonged incubation of cells with YM-58483 during 2 h. It was found that this YM-58483 action did not affect ($P > 0.05$) the response indices (Fig. 3d). These results suggest that the SOC channels are not involved in CMZ action in our experiments.

Contribution of PLA_2 and PLC

CMZ was shown to stimulate Ca^{2+} fluxes into the cytosol through activation of PLA_2 [18–20, 25], with requirement for functional Ca^{2+}-independent phospholipase A_2 ($iPLA_2$) inhibited by CaM [19]. Considering this, we examined the mechanism of CMZ action using PLA_2 inhibitor arachidonyl trifluoromethyl ketone ($AACOCF_3$) also affecting $iPLA_2$ [33] and selective inhibitor of $iPLA_2$, bromoenolactone (BEL). In white adipocytes, adipose-specific PLA_2 (AdPLA) is abundantly expressed, that is sensitive to $AACOCF_3$ and not to BEL, with much lower expression of $iPLA_2$ and other PLA_2s [34, 35]. When 15 μM $AACOCF_3$ was applied in the course of CMZ-induced response, all oscillations ($n = 45$, $N = 31$, 43 and 59) continued, 8.5 ± 1.0% of them ceasing before the end time ($P > 0.05$ vs the data in Fig. 1), so no effect of $AACOCF_3$ was seen. Preincubation with $AACOCF_3$ and the following administration of CMZ showed that all responding cells without exception had a protracted lag of more than 1 min before the first Ca^{2+} spike, reaching the maximum of 10.5 min. No considerable Ca^{2+} rise was obtained during this period indicating that PLA_2 inhibition completely abolished the early Ca^{2+} release typical of control responses. Subsequent Ca^{2+} changes were oscillatory,

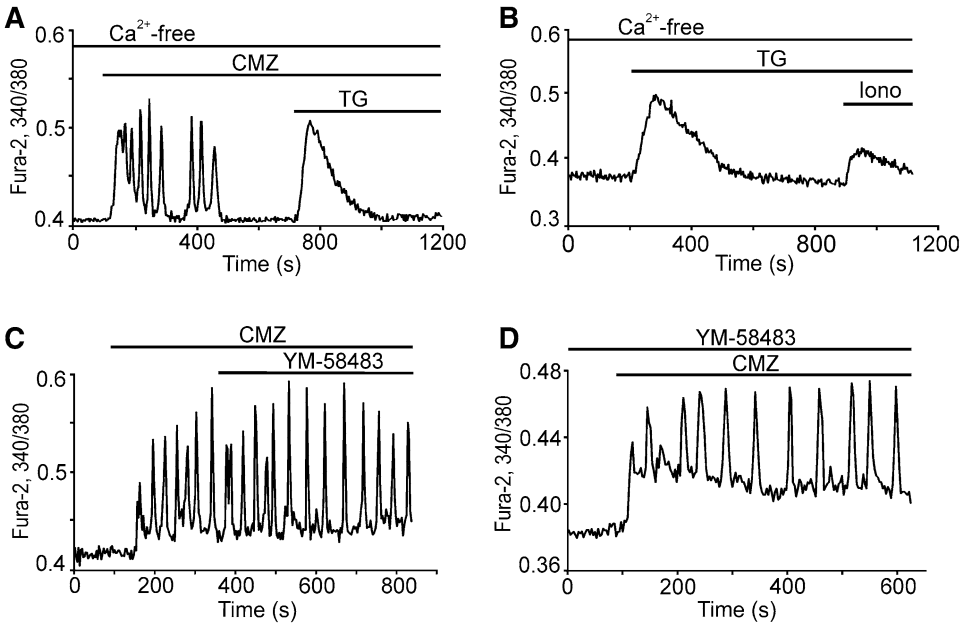

Fig. 3 Ca^{2+} responses upon elimination of Ca^{2+} entry and inhibition of SOC channels. **a** Medium without Ca^{2+} addition but containing 0.5 mM EGTA was applied 30 min before the zero time point. The trace represents $n=111$ from 4 experiments with $N=35–69$, RF = 80.4 ± 11.6%, OF = 59.9 ± 17.9%, LF = 6.0 ± 2.8% ($P>0.05$ for each), where 59.6 ± 28.9% oscillations stopped before the addition of TG ($P<0.05$), compared to Fig. 1. Responses to 10 μM TG averaged in each experiment had the mean amplitude 0.0612 ± 0.0087 fluorescence ratio units and the maximal slope of decline $(2.98 \pm 0.95) \cdot 10^{-4}$ units/s, close ($P>0.05$) to the corresponding values in (**b**). **b** The same zero-Ca^{2+} preincubation as in (**a**), but without CMZ, 5 experiments with $N=32–43$. The amplitude and the slope of responses to 10 μM TG were 0.0792 ± 0.0129 and $(3.26 \pm 0.60) \cdot 10^{-4}$, respectively, and 10 μM ionomycin gave the amplitude of 0.0237 ± 0.0055. **c** Oscillations continue after application of 1 μM YM-58483 as indicated, $n=40$, $N=37$, 46 and 47. Only 9.0 ± 1.8% of oscillations stopped before the end time ($P>0.05$ vs Fig. 1). **d** Preincubation with YM-58483 during 2 h has no effect; oscillations occurred in $n=78$ cells, $N=31$, 45 and 56. RF = 78.8 ± 12.8%, OF = 56.4 ± 13.6%, LF = 25.2 ± 7.0%, and 18.4 ± 3.3% of oscillations ceased, the values differed insignificantly ($P>0.05$) from the control in Fig. 1

with normal percentage and pattern (Fig. 4a). This suggests that PLA_2 products are responsible for the early events of Ca^{2+} mobilization and launching of oscillations, but are not involved in the mechanism of oscillations. When BEL was added 5.5 min prior to incubation with CMZ, no change ($P>0.05$) in RF, OF and LF was found (3 experiments, $N=30–52$) compared to Fig. 1. Therefore, the form $iPLA_2$ does not significantly contribute to CMZ action.

As found previously, CMZ-evoked Ca^{2+} release was prevented with phospholipase C (PLC) inhibition by U73122

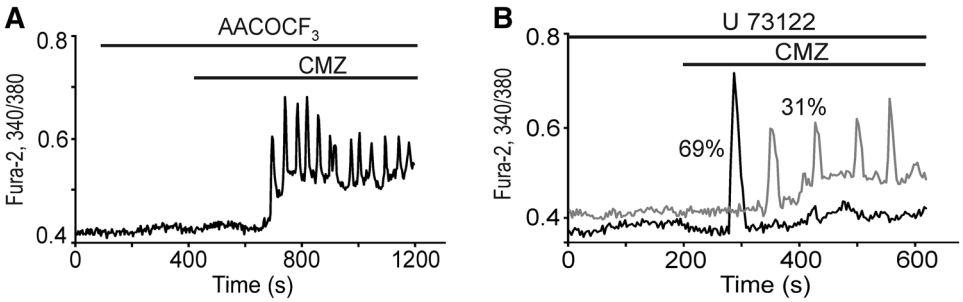

Fig. 4 Effects of PLA_2 (**a**) and PLC (**b**) inhibition. **a** Cells were treated with 15 μM $AACOCF_3$ before CMZ addition, $N=33$, 49 and 50. All responses had the initial lag > 1 min ($n=57$), and one cell with the maximum lag of 10.5 min had no oscillations. RF = 43.8 ± 6.0% and OF = 43.2 ± 6.6% are not significantly different ($P>0.05$) from the control values in Fig. 1. **b** Transient ($n=71$) and oscillations ($n=32$), whose indicated fractions are relative to all 103 responding cells in 3 experiments with $N=54$, 59 and 90. U73122 (10 μM) was added 310 s before time zero. RF = 47.6 ± 9.9%, OF = 17.6 ± 6.7%, LF = 39.57 ± 13.01%, where OF and LF/RF = 79.0 ± 10.0% are significantly different ($P<0.05$) from the control in Fig. 1

[18, 20], or the release was PLC-independent [22]. U73122 also inhibited the non-SOCE pathway [36]. In our experiments, cell incubation with U73122 at the concentration of 10 μM sufficient for the inhibition [18, 20, 36] did not suppress Ca^{2+} responses in general, but modified their prevalent pattern (Fig. 4b). To be exact, oscillations were reduced (OF decreased threefold, $P<0.05$) being replaced by transients, and lag > 1 min before the response, when estimated as LF/RF, increased ($P<0.05$) to 79% and became predominant. Therefore, PLC is not a primary target for CMZ, although PLC activity contributes to both early Ca^{2+} mobilization and subsequent oscillations.

TG-sensitive stores, RyR and IP_3R, acidic stores

To assess significance of the TG-sensitive Ca^{2+} pool in generation of the CMZ-evoked responses, the pool was emptied in Ca^{2+}-free medium prior to CMZ application. It can be seen from Fig. 5a that TG induces a transient with no additional Ca^{2+} release by CMZ, thus indicating that CMZ effect requires the TG-sensitive Ca^{2+} pool to be filled. Addition of Ca^{2+} ionophore ionomycin at the end of the control experiments without CMZ resulted in additional Ca^{2+} release making 30% of the TG-produced amplitude (see Fig. 3b). This demonstrates the existence of a considerable TG-independent pool, which, however, is not engaged by CMZ, at least after emptying the TG-dependent pool. Thus, Ca^{2+} rises and oscillations in adipocytes under CMZ action are totally dependent on organelles accumulating Ca^{2+} via SERCA.

The most recognized routes of stored Ca^{2+} mobilization are IP_3Rs and RyRs of ER [1, 2]. In white adipocytes, RyRs can be activated by an agonist, with their participation being revealed by ryanodine application [27]. Preincubation with this drug at the concentration of 100 μM that locks the channel in a closed state [37] did not eliminate the CMZ-induced oscillations (Fig. 5b). Oscillations also retained (Fig. 5c) in the presence of xestospongin C (XeC), inhibiting IP_3R with $IC_{50}=358$ nM [38]. Simultaneous action of ryanodine and XeC did not lead to any attenuation of oscillations ($n=45$, $N=68$, 500 nM XeC, 100 μM ryanodine) as in the cases of individual treatment. Multiple Ca^{2+} spikes were retained with this mixture in Ca^{2+}-free medium (two experiments with 400 or 500 nM XeC, $n\geq 24$), suggesting no role of

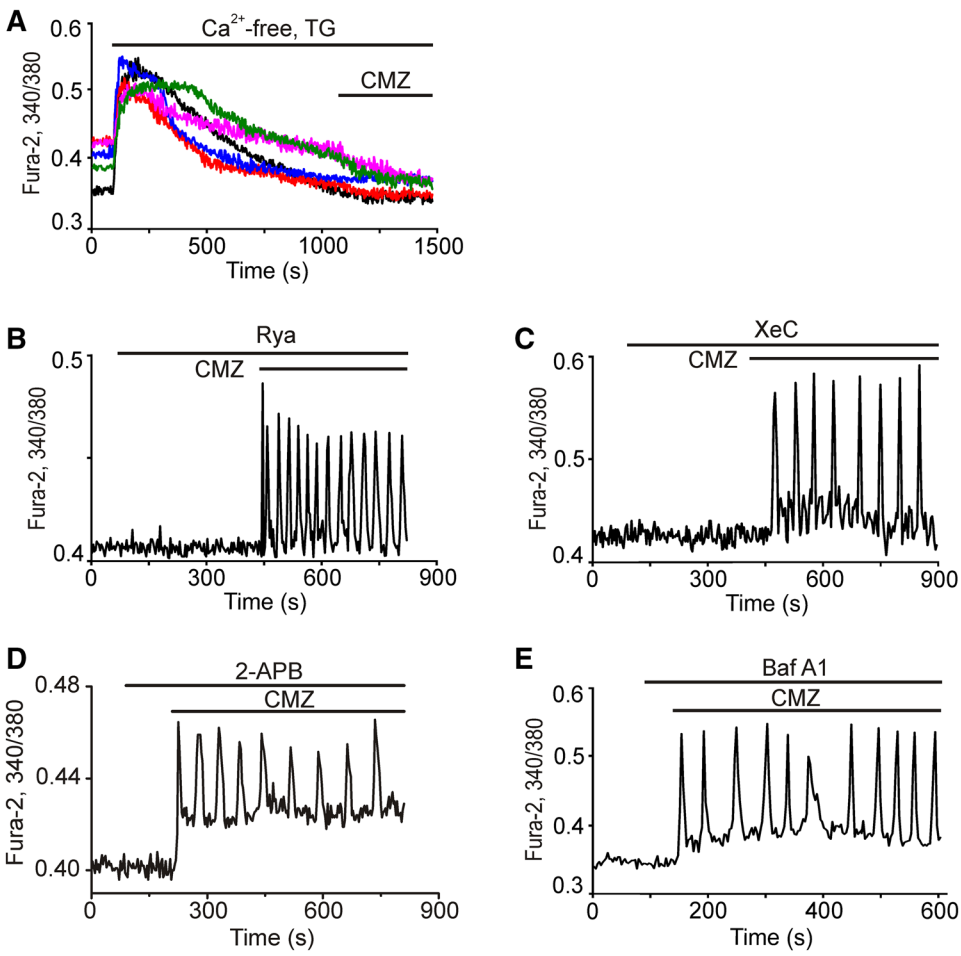

Fig. 5 CMZ-induced Ca^{2+} rises are prevented by discharge of the TG-dependent stores, and oscillations do not require RyR, IP_3R or acidic Ca^{2+} stores. **a** Records for 5 of 68 cells responding to 10 μM TG without Ca^{2+} increase by CMZ, $N=69$. The medium was Ca^{2+}-free from the moment of TG application. No influence of CMZ was observed in a similar experiment with the Ca^{2+}-containing medium ($n=N=48$). **b** $n=21$, $N=53$, RF = 43.4%, 100 μM ryanodine (Rya). **c** $n=42$, $N=68$, RF = 63.2%, 400 nM XeC. **d** 100 μM 2-APB, $N=38$, 46 and 58, RF = 92.5 ± 5.1, OF = 39.6 ± 6.0, with $P<0.01$ and $P>0.05$, correspondingly, vs the data in Fig. 1. Experiments with the same 2-APB addition prior to 10 μM phenylephrine gave RF = 0.011 ± 0.011 ($N=48$, 56 and 58), $P<0.05$ compared to RF = 0.772 ± 0.122 without 2-APB ($N=36$, 56 and 64). **e** 300 nM Baf A1, $n=18$, $N=52$, RF = 44.2%

IP_3Rs and RyRs in short-lived oscillations that arise without Ca^{2+} entry.

At the same time, 400–500 nM XeC applied here may be insufficient for a strong IP_3R suppression, whereas higher doses can inhibit SERCA [39]. For this reason, we complementarily used 2-APB known to inhibit IP_3R [32]. Its efficiency was proved by incubation of cells with 2-APB prior to phenylephrine, an agonist acting through IP_3 production. Such preincubation caused a drastic drop in cell responsiveness to phenylephrine, but did not inhibit CMZ-induced responses: RF even increased due to transients, while OF was unchanged (Fig. 5d). Since 100 μM 2-APB inhibits SOCE [32], our data with the use of 2-APB also indicate that this Ca^{2+} entry pathway is not activated. Remarkably, ARC channels are unaffected by 100 μM 2-APB [40], and their participation, therefore, remains possible.

As to acidic stores, it was previously shown, that 30 s preincubation of white adipocytes with V-ATPase inhibitor, bafilomycin A1 (Baf A1) at 300 nM concentration, eliminated Ca^{2+} increase caused by exogenous NAADP [30]. As seen from Fig. 5e, preincubation with the same concentration of Baf A1 for 60 s did not prevent oscillations evoked by CMZ. Oscillations were also resistant to Baf A1 when its concentration was increased to 1 μM ($n=40$, $N=63$), or preincubation time was extended to 375 s ($n=49$, $N=75$). Cell-permeable antagonist of NAADP, NED-19, added 12 min before CMZ at 100 μM concentration that inhibits calcium spiking in pancreatic β-cells [41], had no effect either ($n=27$, $N=47$).

In adipocytes, calcium signals can be created via activation of CaM-dependent NO-synthase (eNOS), followed by activation of ADP-ribosyl cyclase [28] synthesizing cADPR, NAADP and some other Ca^{2+} active metabolites [12]. To exclude periodic modulation of Ca^{2+} channels by this system, we used the eNOS inhibitor, L-NAME. This inhibitor at 1 mM concentration if applied 6 min before CMZ in Ca^{2+}-free medium together with 100 μM ryanodine and 400 nM XeC, did not influence the CMZ-induced oscillations ($n=34$, $N=66$). Therefore, the oscillations are generated by some kind of intracellular channel that is distinct from RyR, IP_3R and acidic store channels, and is independent of NO.

Connexin and pannexin channels

Connexin and pannexin channels are regulated by several factors including Ca^{2+}, with possible involvement of CaM [10, 13], so they could participate in Ca^{2+} responses to CMZ. We assessed the role of these channels with carbenoxolone (CBX) and octanol. Non-selective inhibitor CBX affects the channels that possess Cx26, Cx30, Cx32, Cx43, Cx46 and Pannexin1 [13]. The effect of CBX was time dependent. After a short preincubation with CBX, cells responded to CMZ by usual oscillations (Fig. 6a). Their premature cessation, characteristic of Ca^{2+} entry abolishment, did not happen, that is the Ca^{2+} entry component dependent on PM hemichannels was not considerable. CBX with Ca^{2+}-free medium allowed for CMZ-induced oscillations (see the legend to Fig. 6a), showing explicitly that their intracellular source was not inhibited by the short-term action of CBX. Longer preincubation (35 min) restrained oscillations in the following way: most cells displayed a single initial pulse (Fig. 6b, black trace), and the others demonstrated the same pulse, which, after a certain period of silence, was accompanied with oscillations, mainly with a low amplitude (Fig. 6b, grey trace). Two-hour preincubation with CBX (Fig. 6c) did not significantly lower cell responsiveness, while oscillations were strongly inhibited ($P<0.0001$). The influence of CBX was not caused by the inhibition of Ca^{2+} entry supporting oscillations, since there were no oscillations just after the first peak, in contrast to their existence in the Ca^{2+}-free medium. To verify and specify these results, we also applied octanol that inhibits Cx38, Cx43, and Cx50, with no reported action on pannexins [13]. Two-hour preincubation with octanol gave the same results as with CBX. Namely, responsiveness to CMZ was retained suggesting the fullness of the CMZ-sensitive stores, and the responses had the form of transients without oscillations (Fig. 6d). Subsequent addition of TG typically increased the level of Ca^{2+} ($N=35$ and $N=41$), revealing non-empty stores. We supposed, therefore, that the suppressive effect of prolonged preincubation with CBX or octanol was due to the postponed inhibition of connexons in the intracellular structures. Remaining CBX-independent initial spikes are evidently of another origin related to activation of phospholipases (see above).

Possible ATP secretion through PM hemichannels causing the stimulation of $P2Y_2$ receptors and Ca^{2+} increase in adipocytes [42] prompted us to test the contribution of this pathway. Cell treatment with 5 U/mL hexokinase before CMZ had no effect on both the initial Ca^{2+} release and subsequent oscillations ($N=63$), implicating that such ATP secretion plays no role in the observed responses.

Effect of La^{3+}

Lanthanides La^{3+} and Gd^{3+} block channels for Ca^{2+} entry into the cell, affecting SOC and, at higher concentrations, non-SOC channels [5, 32, 36]. In particular, it was demonstrated that ARC channels [40, 43] and Cx43 hemichannels [44] can be inhibited by these ions, which gave us grounds to expect an action covering both $AACOCF_3$ and CBX/octanol effects. La^{3+}does not permeate the cells and blocks Ca^{2+} entry by acting extracellularly [45], so we supposed that La^{3+} could be used to reveal the role of the PM Ca^{2+} channels located in endocytic vesicles and in organelles to which these La^{3+}-containing vesicles are fused. Taking into

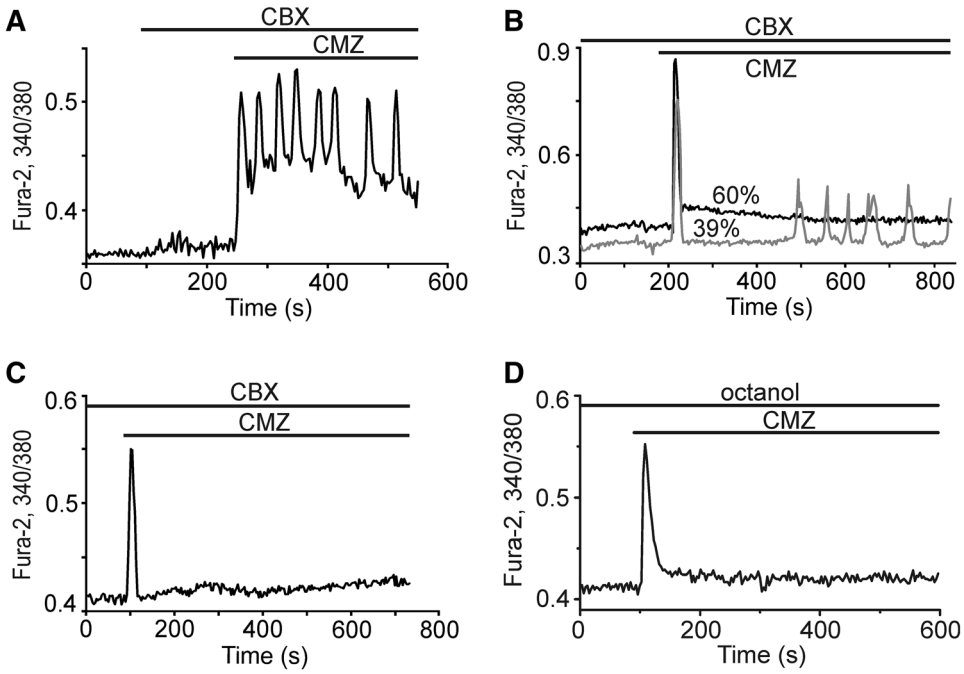

Fig. 6 Responses to CMZ after preincubation of adipocytes with CBX and octanol. Cells were exposed to 100 μM CBX or 1 mM octanol as indicated (**a**), or starting from 35 min (**b**) and 2 h (**c, d**) before time zero. **a** $n=12$ (1 stopped), $N=47$, RF = 34.0%. In another experiment with Ca^{2+}-free medium applied together with CBX, and CMZ added 156 s later, oscillations occurred with $n=30$ (10 stopped), $N=64$, RF = 50.0%. **b** $n=60$ (black trace), $n=39$ (gray trace), percents at the traces relative to 100 responding cells, one of which demonstrated delayed oscillations without the initial pulse. $N=110$, RF = 90.9%. **c** Example typical of 3 experiments, $n=11$, 15 and 16, $N=31$, 39 and 39. Oscillations remained in 7 cells, including 5 cells with small amplitudes. RF = 44.3 ± 4.7% ($P>0.05$) and OF = 6.0 ± 3.7% ($P<0.0001$), where P is determined relative to the control in Fig. 1. **d** $N=35$, 41 and 43, RF = 61.8 ± 17.7, OF = 6.2 ± 2.7 ($P<0.0001$ vs Fig. 1)

account the characteristic time of the endocytic transport that can reach 1–2 h [46] and the obtained development of CBX inhibition on the same time scale, preincubation of adipocytes with La^{3+} was performed for 30 min, two and 24 h.

Incubation with 1 mM La^{3+} for 30 min resulted in partial deterioration of oscillations, as exemplified by a complex transient in Fig. 7a. Although responsiveness decreased insignificantly, oscillations were sensitive to La^{3+} inasmuch as the fraction of oscillations in responses decreased by 1/3 with $P<0.001$. Only about 1/4 of the remaining oscillations were rather regular and prolonged. Subsequent addition of TG to the Ca^{2+}-free medium evoked Ca^{2+} rise in all tested cells ($N=42$ and 45) with an amplitude comparable to the foregoing peaks, similar to those shown in Fig. 3a. Prolongation of the preincubation time to 2 h led to strong inhibition of Ca^{2+} responses (Fig. 7b). Response and oscillation indices decreased by 74.3% ($P<0.01$) and 86.9% ($P<0.0001$), respectively. This effect was not a result of depletion of Ca^{2+} stores, since subsequent TG addition together with Ca^{2+}-free medium again produced usual response amplitudes (not shown).

To estimate the maximal La^{3+} effect and to exclude emptying of stored Ca^{2+} more reliably, the culture was incubated with La^{3+} for 24 h. The preincubation did not change vitality of cells and their morphology. Like with a shorter 2-h preincubation (Fig. 7b), the La^{3+} presence during 24 h inhibited responses to CMZ almost completely, leaving them in only 2 of 112 analyzed cells (Fig. 7c). Importantly, subsequent responses to TG and ionomycin, applied in Ca^{2+}-free medium, retained, demonstrating the fullness of the Ca^{2+} stores. Statistical comparison showed that Ca^{2+} responsiveness to CMZ dropped at $P<0.05$, while the TG-induced response amplitude even increased, although insignificantly (Fig. 7d). Thus, the lack of signals after the long-lasting La^{3+} presence is not a consequence of reduced internal stores determining the Ca^{2+} release by CMZ. From Ca^{2+} decline in Fig. 7c, it can be deduced that PMCA was not blocked by La^{3+}. Note that 24-h exposition of adipocytes to La^{3+} slightly decreased ($P<0.05$) the fluorescence intensity of unstimulated cells (Fig. 7d). Consequently, La^{3+} able to change the fura-2 fluorescence excitation spectrum similar to Ca^{2+} [45] did not permeate into the cytosol and did not accumulate in it during this period, thus indicating the organellar localization of La^{3+} and its targets. Despite the possible interaction of La^{3+} with multivalent anions in the solution [32], its amount was *de facto* enough to inhibit Ca^{2+} rises.

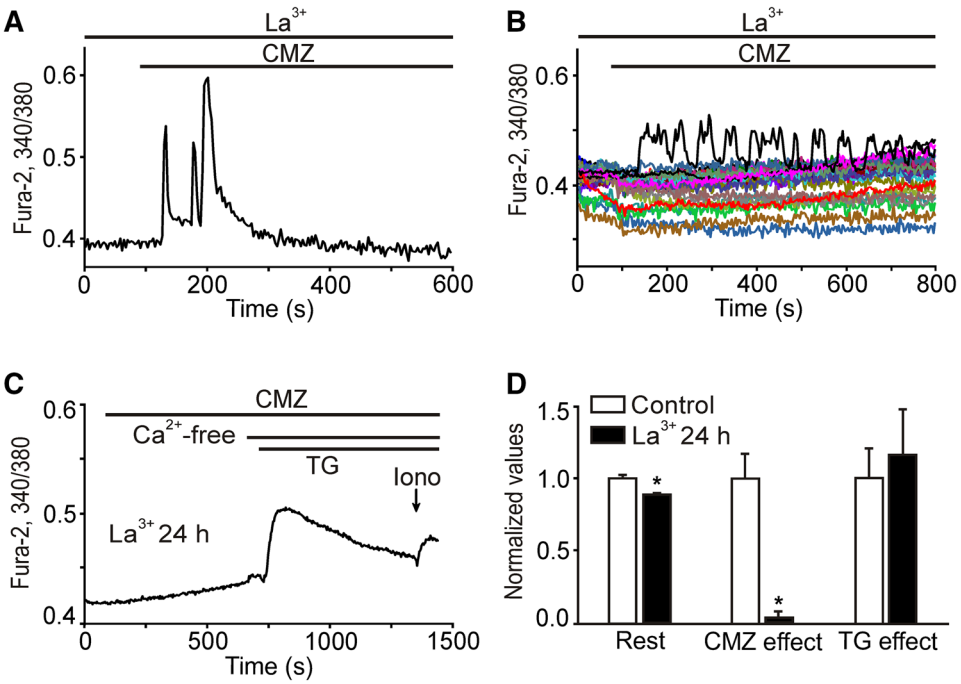

Fig. 7 Treatment of adipocytes with La^{3+} for increased time periods suppresses Ca^{2+} responses to CMZ without reducing Ca^{2+} stores. Preincubation with 1 mM La^{3+} for 30 min (**a**), 2 h (**b**) and 24 h (**c** and **d**). 10 µM TG and 1 µM ionomycin (Iono) were used. *P* values in (**a, b**) are determined relative to the data in Fig. 1. **a** A representative response deviating from typical oscillations. In three experiments, $n=64$ (any responses), $N=42$, 45 and 59, RF = 44.5 ± 6.5% ($P>0.05$), OF = 28.3 ± 6.8% ($P<0.005$), OF/RF = 63.8 ± 2.4 ($P<0.001$). **b** Traces of 25 out of the 59 non-responding cells (for clarity, the remaining traces are not presented) and only one response in the experiment with $N=60$. In all 4 experiments, $N=23$, 29, 33 and 60, RF = 14.7 ± 7.5 ($P<0.01$) and OF = 7.1 ± 4.0 ($P<0.0001$). **c** Time course of the mean Ca^{2+} level, based on 3 experiments with $N=36$, 37 and 39, where only 2 cells responded to CMZ, both with oscillations. **d** Resting Ca^{2+} level (Rest), RF for CMZ (CMZ effect), and the amplitude of the TG-evoked responses (TG effect) for experiments of panel (**c**) in comparison with control without La^{3+}. *$P<0.05$. Values are normalized to the mean in the control ($N=31$, 40, 42), for which RF = 41.8 ± 7.2%, the fura-2 ratio at rest is 0.473 ± 0.013, and the amplitude measured from the averaged (including oscillations) level is 0.0577 ± 0.0113, the same ($P>0.05$) as the amplitude in Fig. 3a

It was found that endocytosis is negligible below 10 °C [47]. Given this, low temperature should block La^{3+} delivery to intracellular structures and restore Ca^{2+} responses to CMZ. Storage of adipocytes at 4 °C for 1 h (not more) preserved cell vitality, and RF = 90.2% and OF = 60.3% were obtained for La^{3+}-treated cells (the mean of two experiments with $N=30$ and $N=47$). These values are 2 and 2.1 times higher than the corresponding values for the cells incubated with La^{3+} at normal temperature during even a shorter period of time (30 min, Fig. 7a). We consider this increase of responsiveness as a support of the proposal that CMZ-induced responses depend on organelle-located PM calcium channels accessible to the inhibitor by endocytosis.

Discussion

Our experiments revealed that CMZ interfering with CaM-dependent regulation of Ca^{2+} fluxes initiates persistent oscillations of the cytosolic Ca^{2+} concentration by activating both Ca^{2+} release and entry. The oscillations existed in a rather wide range of 2.5–10 µM CMZ, with no responses in any cell at 1 µM and with reduction of this mode at 10 µM. The same threshold action of low CMZ concentrations on the Ca^{2+} level was observed in other cell types, with similar [17, 18, 20] or higher sensitivity [22] to CMZ. Decaying oscillations in response to 10 µM CMZ were previously obtained in HeLa cells, but only in Ca^{2+}-free medium, leading to the conclusion that Ca^{2+} entry did not support, but rather compromised oscillations [20]. Our results with and without Ca^{2+} in the medium have shown that Ca^{2+} entry positively influences the intracellularly generated oscillations by maintaining them.

Phospholipases PLA_2 and PLC, both capable to supply AA had different effects on responses to CMZ. The early Ca^{2+} release was provided mainly by PLA_2, but the subsequent oscillations were partially dependent on PLC and not on PLA_2. The ability of exogenous AA to evoke Ca^{2+} release [20], non-SOCE activation [20, 36, 48] and Ca^{2+} response in adipocytes [25], as well as CMZ action not requiring AA-derived metabolites [20], suggests that effects of phospholipases in our data implicated direct activation of ARC

channels by AA. Nevertheless, the action on the same channels through LTC_4 [5] is not excluded. This activation is in line with the observed here attenuation of responses to CMZ after incubation with La^{3+} inhibiting ARC [43] among other channels. Lowering the AA level by PLA_2 inhibition resulted in oscillations emerging with a delay, which could reflect weak AA-induced Ca^{2+} release and slow (within minutes) development of the CMZ effect on connexons responsible for oscillatory Ca^{2+} release. The influence of PLC on Ca^{2+} responses was not related to the IP_3-mediated Ca^{2+} release, because no IP_3R impact was detected, and early Ca^{2+} rise strongly depended on PLA_2 functioning. This suggests the involvement of the second PLC product, diacylglycerol (DAG). Upon DAG accumulation, AA can be produced by DAG lipase, resulting in activation of non-SOCE [36]. Given that PLC shortened the initial lag in adipocytes, although less efficiently than PLA_2, it is possible that CMZ released Ca^{2+} partially due to the AA formation by DAG lipase. The subsequent oscillations seem to depend on DAG-derived AA, with the much less contribution of AA made at this phase by PLA_2. The absence of BEL effect, consistent with insignificant expression of $iPLA_2$ in adipocytes [35], implies that CMZ could activate AdPLA, conceivably by antagonizing its inhibition by CaM.

No influence of SOC channels on Ca^{2+} responses to 5 µM CMZ was found here using YM-58483 or 2-APB, so the entire entry was represented by non-SOCE. This fact is likely a consequence of insignificant decrease in stored Ca^{2+} content indicated by subsequent full-size TG responses. Moreover, our data agree with vast predominance of non-SOCE at [CMZ] ≥ 5 µM [17, 19, 20, 48] and SOCE attenuation by CMZ [15], probably caused by accumulation of AA that activates non-SOCE and inhibits SOCE [48]. Since there are evidences for YM-58483 [49] and 2-APB [50] action on several TRP family channels, our negative results with these inhibitors argue against the contribution of this channel type to Ca^{2+} entry and oscillations initiated by CMZ.

Non-involvement of IP3R or RyR in our results complies with Ca^{2+} release by CMZ at inhibited PLC [22] and atypical CICR not requiring these channels [51] found in living cells. In search for an alternative source of the CMZ-induced oscillations, our key finding was that sufficiently prolonged incubation of the culture with La^{3+}, inhibiting Ca^{2+} entry channels, prevented Ca^{2+} responses, including Ca^{2+} release. We interpret this deferred action as a non-permeable inhibitor reaching its organelle-located targets through endocytosis. The subcellular presence of PM channels typically serving for Ca^{2+} entry is exemplified by Orai1, whose constitutive recycling between PM and endosomes provides a considerable percentage of total Orai1 in these organelles [52]. According to our results, neither PM-located, nor organellar Orai1-containing SOC channels play a role in the CMZ-induced responses, as seen from the incubation with YM-58483 up to 2 h. This drug does not permeate through the cell membrane during 24-h preincubation [31], but it could be uptaken and passed to organelles like La^{3+}. Therefore, La^{3+}-sensitive organellar channels distinct from CRAC channels were involved, which could be ARC channels and connexons. It is important that even 24-h incubation with La^{3+} did not empty the intracellular Ca^{2+} pools, thus rejecting the unresponsiveness of adipocytes as a simple consequence of this pool loss. This resistance to depletion may stem from La^{3+}-inhibition of virtually all Ca^{2+} entry channels, including those in organelles, together with lowering the PMCA activity at the normal resting Ca^{2+} level and below it.

Intracellular connexons seem to be most closely related to the mechanism of oscillations, since their inhibition by prolonged incubation with CBX or octanol effectively abolished oscillations leaving the initial transient, and inhibition by La^{3+} suppressed all responses, including oscillations. Similar to our data, 30-min preincubation with CBX suppressed bradykinin-induced oscillation, but left the initial peak in MDCK cells expressing Cx32 and Cx43 [8]. It was concluded that hemichannels contribute to the IP_3R-based oscillations [8], and involvement of Cx43 hemichannels was specified [9]. Cx43 channels are common targets for CBX and octanol [13], and they are also inhibited by La^{3+} [44], so the three lines of evidence converge on the Cx43 isoform to be responsible for Ca^{2+} oscillations studied here. These connexons could transport an intracellular messenger triggering oscillations through another Ca^{2+} channel, but our data ruled out participation of evident candidates, such as NAADP, acidic stores or IP_3R and RyR. On the other hand, the bell-shaped Ca^{2+} influence on the Cx43 hemichannel opening was shown based on ATP release, and such Ca^{2+} effect was also observed at the single channel level in the patch-clamp experiments [10]. We propose, therefore, a more straightforward possibility of CICR arising from Ca^{2+} release through organellar connexons and activation of just these channels. The bell-shaped Ca^{2+} dependence of Cx43 connexons can be sufficient for the steady state instability and appearance of oscillations, as shown for IP_3R [53] with the same dependence character. CMZ presumably initiates oscillations by evoking the production of AA that releases Ca^{2+} through AA-activated channels causing CICR through intracellular connexons, and AA may also promote [10] the opening of connexons. The lag preceding oscillations may reflect the time required for the subthreshold accumulation of activating Ca^{2+}, AA or AA-derived intermediates. The rapid cessation of Ca^{2+} oscillations after blocking the hemichannels [7–9], that did not occur in our results, is consistent with a minor role of PM hemichannels in the cultured adipocytes in respect to CMZ-evoked Ca^{2+} changes. The processes able to account for the data of the present work are summarized in Fig. 8.

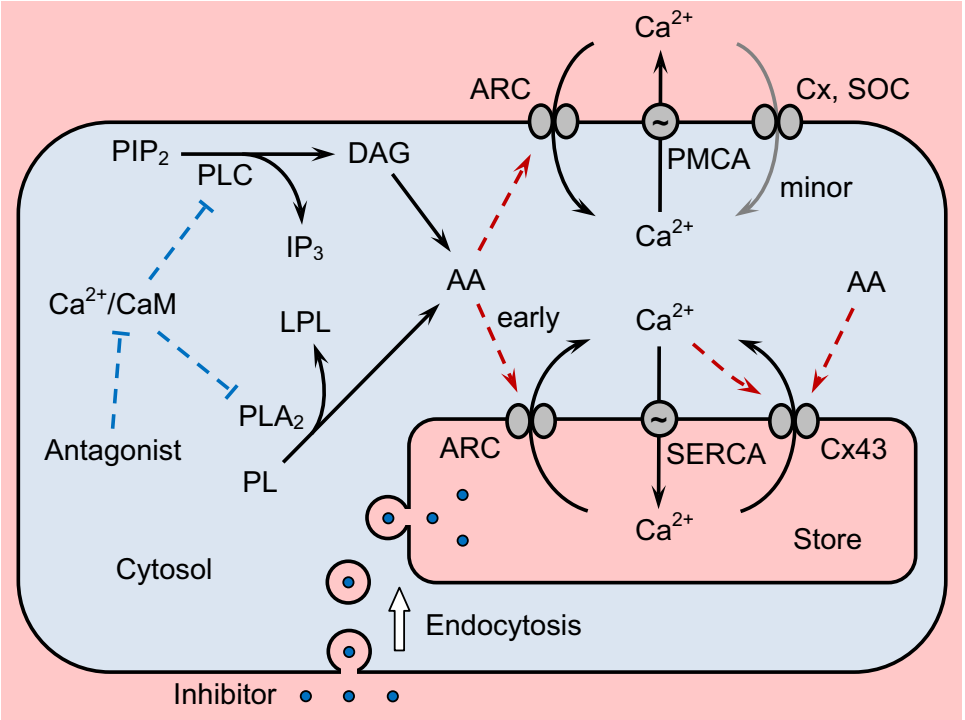

Fig. 8 Scheme of CaM-mediated regulation of Ca^{2+} fluxes in adipocytes inferred from the obtained results. One generalized compartment with SERCA and both Ca^{2+}-releasing channels is provisionally shown, but these channels may also be located in different organelles. Dashed arrows with sharp and T-shaped ends stand for activation and inhibition, which can proceed via intermediate steps. PIP_2: phosphatidylinositol 4,5-bisphosphate, PL: phospholipid, LPL: lysophospholipid. All other abbreviations and explanations are given in the text

As for organellar identity of Ca^{2+} pools that generate oscillations under CMZ action, several versions can be considered. The dependence of responses on SERCA pumping points to the SERCA-possessing organelles, in particular ER, as the main source of CMZ-releasable Ca^{2+}. Meanwhile, the effect of TG can also be indirect, in the sense that a massive TG-induced Ca^{2+} release could merely discharge other organelles not equipped with SERCA, and therefore, prevent subsequent Ca^{2+} rises by CMZ. A candidate for the generator role is the Golgi apparatus that contains SERCA in the cis and medial sections [54], and also incorporates oligomerized connexins derived (as monomers in the case of Cx43) from ER [11]. Trans-Golgi and secretory vesicles, accumulating Ca^{2+} via the secretory pathway Ca^{2+}-ATPase, can possess RyRs allowing for CICR [54], so these stores may represent the case of indirect TG dependence. Trafficking of the PM-derived endosomes could explain the long delay in the effect of Ca^{2+} entry inhibitors as the time needed to deliver the extracellular solution through the vesicles to the intracellular structures capable of oscillations. In this process, the endosomal cargo can reach the trans-Golgi network owing to bidirectional vesicle exchange [55] and then pass to other compartments. Endosomes themselves contain internalized Cx [11], and probably, ARC channels, although their Ca^{2+} is lost within minutes to few μM, in parallel with acidification [56]. Specialized GLUT4 storage vesicles in adipocytes may contain V-ATPase, and therefore, belong to acidic compartments [57], apparently not involved in the present study. Nevertheless, Ca^{2+} transport in these vesicles should be characterized in more detail, and their role in the responses is still possible.

CaM antagonists have some non-specific effects not mediated by CaM, of which direct inhibition of SERCA [58] might be the most relevant to our data. However, disparate IC_{50} values for CMZ and TFP were reported [58] in contrast to that similar oscillations were observed here at the same concentrations of either CMZ or TFP. Besides, SERCA was not inhibited by CMZ judging from the conserved Ca^{2+} stores after CMZ action.

Targeted inhibition of CaM has shown that this protein is essential for cell viability and proliferation. Accordingly, CaM antagonists arrest proliferation and induce apoptosis of tumor cells, which makes promising their use for therapeutic purpose. Anti-CaM drugs could also exert protective effect on non-transformed cells, such as neurones, cardiomyocytes, β-cells, and cells of the immune system, in cases when CaM has proapoptotic function [3]. Since Ca^{2+} overload can cause cell death by various ways [1, 3], Ca^{2+} behavior under such treatments becomes an important factor. We showed that, starting at a critical dose, CaM antagonist can destabilize Ca^{2+} homeostasis and produce oscillations. This regime is not necessarily deleterious for cells, because the Ca^{2+} rises are of short duration. Cytotoxicity could be related rather to large Ca^{2+} transients, caused by the abrupt drug action on the cell, as well as to strong permanent Ca^{2+} elevations because of the excessive stimulation of PLA_2, PLC and downstream ARC and Cx channels. Therefore, our results can be useful in developing strategies for selection

and administration of anti-CaM drugs, possibly in combination with agents reducing AA impact, to control viability and correct abnormal functions of adipocytes and other cells.

In conclusion, CaM mediates regulation of the Ca^{2+} level in white adipocytes, and alleviation of this regulation leads to Ca^{2+} transients and sustained oscillations. The underlying mechanism implicates control of AA-activated and connexin channels by phospholipases A_2 and C via their products (AA, DAG) distinct from IP_3. Organellar connexons appear to play an essential role in the oscillations and may generate them due to own CICR. Operation of this phosholipase-triggered mechanism may be not limited by the conditions of weakened CaM regulation, and its involvement in agonist-induced Ca^{2+} signaling is plausible.

Acknowledgements This work was supported by a Grant of the President of the Russian Federation (Ref: MK-626.2018.4, EAT).

Author contributions EAT performed all experiments, contributed to the experimental design and data analysis and prepared figures. VPZ contributed reagents and materials, participated in the discussion of results, and edited the manuscript. NPK conceived the study, designed the experiments, analyzed and interpreted the data, and wrote the manuscript.

Compliance with ethical standards

Conflict of interest The authors state that they have no conflict of interest pertaining to this manuscript.

References

1. Carafoli E, Santella L, Brance D, Brini M (2001) Generation, control, and processing of cellular calcium signals. Crit Rev Biochem Mol Biol 36:107–260
2. Berridge MJ (2012) Calcium signalling remodelling and disease. Biochem Soc Trans 40:297–309
3. Berchtold MW, Villalobo A (2014) The many faces of calmodulin in cell proliferation, programmed cell death, autophagy, and cancer. Biochim Biophys Acta 1843:398–435
4. Uhlén P, Fritz N (2010) Biochemistry of calcium oscillations. Biochem Biophys Res Commun 396:28–32
5. Trebak M, Putney JW Jr (2017) ORAI calcium channels. Physiology (Bethesda) 32:332–342
6. Shuttleworth TJ (1999) What drives calcium entry during $[Ca^{2+}]_i$ oscillations?—challenging the capacitative model. Cell Calcium 25:237–246
7. Kawano S, Otsu K, Kuruma A, Shoji S, Yanagida E, Muto Y, Yoshikawa F, Hirayama Y, Mikoshiba K, Furuichi T (2006) ATP autocrine/paracrine signaling induces calcium oscillations and NFAT activation in human mesenchymal stem cells. Cell Calcium 39:313–324
8. De Bock M, Wang N, Bol M, Decrock E, Ponsaerts R, Bultynck G, Dupont G, Leybaert L (2012) Connexin 43 hemichannels contribute to cytoplasmic Ca^{2+} oscillations by providing a bimodal Ca^{2+}-dependent Ca^{2+} entry pathway. J Biol Chem 287:12250–12266
9. Bol M, Wang N, De Bock M, Wacquier B, Decrock E, Gadicherla A, Decaluwé K, Vanheel B, van Rijen HV, Krysko DV, Bultynck G, Dupont G, Van de Voorde J, Leybaert L (2017) At the cross-point of connexins, calcium, and ATP: blocking hemichannels inhibits vasoconstriction of rat small mesenteric arteries. Cardiovasc Res 113:195–206
10. Leybaert L, Lampe PD, Dhein S, Kwak BR, Ferdinandy P, Beyer EC, Laird DW, Naus CC, Green CR, Schulz R (2017) Connexins in cardiovascular and neurovascular health and disease: pharmacological implications. Pharmacol Rev 69:396–478
11. Laird DW (2006) Life cycle of connexins in health and disease. Biochem J 394:527–543
12. Bruzzone S, Guida L, Sturla L, Usai C, Zocchi E, De Flora A (2012) Subcellular and intercellular traffic of NAD^+, NAD^+ precursors and NAD^+-derived signal metabolites and second messengers: old and new topological paradoxes. Messenger 1:34–52. https://doi.org/10.1166/msr.2012.1007
13. D'hondt C, Ponsaerts R, De Smedt H, Bultynck G, Himpens B (2009) Pannexins, distant relatives of the connexin family with specific cellular functions? Bioessays 31:953–974
14. Morgan AJ, Platt FM, Lloyd-Evans E, Galione A (2011) Molecular mechanisms of endolysosomal Ca^{2+} signalling in health and disease. Biochem J 439:349–374
15. Tornquist K, Ekokoski E (1996) Inhibition of agonist-mediated calcium entry by calmodulin antagonists and by the Ca^{2+}/calmodulin kinase II inhibitor KN-62. Studies with thyroid FRTL-5 cells. J Endocrinol 148:131–138
16. Watanabe H, Takahashi R, Tran QK, Takeuchi K, Kosuge K, Satoh H, Uehara A, Terada H, Hayashi H, Ohno R, Ohashi K (1999) Increased cytosolic Ca^{2+} concentration in endothelial cells by calmodulin antagonists. Biochem Biophys Res Commun 265:697–702
17. Harper JL, Daly JW (2000) Effect of calmidazolium analogs on calcium influx in HL-60 cells. Biochem Pharmacol 60:317–324
18. Jan CR, Tseng CJ (2000) Calmidazolium-induced rises in cytosolic calcium concentrations in Madin-Darby canine kidney cells. Toxicol Appl Pharmacol 162:142–150
19. Smani T, Zakharov SI, Csutora P, Leno E, Trepakova ES, Bolotina VM (2004) A novel mechanism for the store-operated calcium influx pathway. Nat Cell Biol 6:113–120
20. Peppiatt CM, Holmes AM, Seo JT, Bootman MD, Collins TJ, McDonald F, Roderick HL (2004) Calmidazolium and arachidonate activate a calcium entry pathway that is distinct from store-operated calcium influx in HeLa cells. Biochem J 381:929–939
21. Zinchenko VP, Kasymov VA, Li VV, Kaimachnikov NP (2005) The calmodulin inhibitor R24571 induces a short-term Ca^{2+} entry and a pulse-like secretion of ATP in Ehrlich ascites tumor cells. Biofizika 50:1055–1069
22. Liao WC, Huang CC, Cheng HH, Wang JL, Lin KL, Cheng JS, Chai KL, Hsu PT, Tsai JY, Fang YC, Lu YC, Chang HT, Huang JK, Chou CT, Jan CR (2009) Effect of calmidazolium on $[Ca^{2+}]_i$ and viability in human hepatoma cells. Arch Toxicol 83:61–68
23. Somogyi R, Stucki JW (1991) Hormone-induced calcium oscillations in liver cells can be explained by a simple one pool model. J Biol Chem 266:11068–11077
24. Uneyama H, Uneyama C, Akaike N (1993) Intracellular mechanisms of cytoplasmic Ca^{2+} oscillation in rat megakaryocyte. J Biol Chem 268:168–174
25. Turovsky EA, Kaimachnikov NP, Zinchenko VP (2014) Agonist-specific participation of SOC and ARC channels and $iPLA_2$ in the regulation of Ca^{2+} entry during oscillatory responses in adipocytes. Biochem (Moscow) Suppl Ser A: Membr Cell Biol 8:136–143. https://doi.org/10.1134/S1990747813050206
26. Veigl ML, Klevit RE, Sedwick WD (1989) The uses and limitations of calmodulin antagonists. Pharmacol Ther 44:181–239
27. Turovsky EA, Kaimachnikov NP, Turovskaya MV, Berezhnov AV, Dynnik VV, Zinchenko VP (2012) Two mechanisms of calcium oscillations in adipocytes. Biochem (Moscow) Suppl Ser A:

Membr Cell Biol 6:26–34. https://doi.org/10.1134/S1990747810601 6X
28. Dolgacheva LP, Turovskaya MV, Dynnik VV, Zinchenko VP, Goncharov NV, Davletov B, Turovsky EA (2016) Angiotensin II activates different calcium signaling pathways in adipocytes. Arch Biochem Biophys 593:38–49
29. Bogan SJ (2012) Regulation of glucose transporter translocation in health and diabetes. Annu Rev Biochem 81:507–532
30. Park KH, Kim BJ, Shawl AI, Han MK, Lee HC, Kim UH (2013) Autocrine/paracrine function of nicotinic acid adenine dinucleotide phosphate (NAADP) for glucose homeostasis in pancreatic β-cells and adipocytes. J Biol Chem 288:35548–35558
31. Zitt C, Strauss B, Schwarz EC, Spaeth N, Rast G, Hatzelmann A, Hoth M (2004) Potent inhibition of Ca^{2+} release-activated Ca^{2+} channels and T-lymphocyte activation by the pyrazole derivative BTP2. J Biol Chem 279:12427–12437
32. Putney JW (2010) Pharmacology of store-operated calcium channels. Mol Interv 10:209–218
33. Ackermann EJ, Conde-Frieboes K, Dennis EA (1995) Inhibition of macrophage Ca^{2+}-independent phospholipase A_2 by bromoenol lactone and trifluoromethyl ketones. J Biol Chem 270:445–450
34. Duncan RE, Sarkadi-Nagy E, Jaworski K, Ahmadian M, Sul HS (2008) Identification and functional characterization of adipose-specific phospholipase A_2 (AdPLA). J Biol Chem 283:25428–25436
35. Jaworski K, Ahmadian M, Duncan RE, Sarkadi-Nagy E, Varady KA, Hellerstein MK, Lee HY, Samuel VT, Shulman GI, Kim KH, de Val S, Kang C, Sul HS (2009) AdPLA ablation increases lipolysis and prevents obesity induced by high-fat feeding or leptin deficiency. Nat Med 15:159–168
36. Broad LM, Cannon TR, Taylor CW (1999) A non-capacitative pathway activated by arachidonic acid is the major Ca^{2+} entry mechanism in rat A7r5 smooth muscle cells stimulated with low concentrations of vasopressin. J Physiol 517:121–134
37. Zimányi I, Buck E, Abramson JJ, Mack MM, Pessah IN (1992) Ryanodine induces persistent inactivation of the Ca^{2+} release channel from skeletal muscle sarcoplasmic reticulum. Mol Pharmacol 42:1049–1057
38. Gafni J, Munsch JA, Lam TH, Catlin MC, Costa LG, Molinski TF, Pessah IN (1997) Xestospongins: potent membrane permeable blockers of the inositol 1,4,5-trisphosphate receptor. Neuron 19:723–733
39. Castonguay A, Robitaille R (2002) Xestospongin C is a potent inhibitor of SERCA at a vertebrate synapse. Cell Calcium 32:39–47
40. Mignen O, Thompson JL, Shuttleworth TJ (2003) Ca^{2+} selectivity and fatty acid specificity of the noncapacitative, arachidonate-regulated Ca^{2+} (ARC) channels. J Biol Chem 278:10174–10181
41. Naylor E, Arredouani A, Vasudevan SR, Lewis AM, Parkesh R, Mizote A, Rosen D, Thomas JM, Izumi M, Ganesan A, Galione A, Churchill GC (2009) Identification of a chemical probe for NAADP by virtual screening. Nat Chem Biol 5:220–226
42. Lee H, Jun DJ, Suh BC, Choi BH, Lee JH, Do MS, Suh BS, Ha H, Kim KT (2005) Dual roles of P2 purinergic receptors in insulin-stimulated leptin production and lipolysis in differentiated rat white adipocytes. J Biol Chem 280:28556–28563
43. Mignen O, Shuttleworth TJ (2000) I_{ARC}, a novel arachidonate-regulated, noncapacitative Ca^{2+} entry channel. J Biol Chem 275:9114–9119
44. John SA, Kondo R, Wang SY, Goldhaber JI, Weiss JN (1999) Connexin-43 hemichannels opened by metabolic inhibition. J Biol Chem 274:236–240
45. Kwan CY, Putney JW Jr (1990) Uptake and intracellular sequestration of divalent cations in resting and methacholine-stimulated mouse lacrimal acinar cells. Dissociation by Sr^{2+} and Ba^{2+} of agonist-stimulated divalent cation entry from the refilling of the agonist-sensitive intracellular pool. J Biol Chem 265:678–684
46. Sorkin A, von Zastrow M (2002) Signal transduction and endocytosis: close encounters of many kinds. Nat Rev Mol Cell Biol 3:600–614
47. Weigel PH, Oka JA (1981) Temperature dependence of endocytosis mediated by the asialoglycoprotein receptor in isolated rat hepatocytes. Evidence for two potentially rate-limiting steps. J Biol Chem 256:2615–2617
48. Holmes AM, Roderick HL, McDonald F, Bootman MD (2007) Interaction between store-operated and arachidonate-activated calcium entry. Cell Calcium 41:1–12
49. He LP, Hewavitharana T, Soboloff J, Spassova MA, Gill DL (2005) A functional link between store-operated and TRPC channels revealed by the 3,5-bis(trifluoromethyl)pyrazole derivative, BTP2. J Biol Chem 280:10997–11006
50. Bodendiek SB, Raman G (2010) Connexin modulators and their potential targets under the magnifying glass. Curr Med Chem 17:4191–4230
51. Beauvois MC, Arredouani A, Jonas JC, Rolland JF, Schuit F, Henquin JC, Gilon P (2004) Atypical Ca^{2+}-induced Ca^{2+} release from a sarco-endoplasmic reticulum Ca^{2+}-ATPase 3-dependent Ca^{2+} pool in mouse pancreatic beta-cells. J Physiol 559:141–156
52. Yu F, Sun L, Machaca K (2010) Constitutive recycling of the store-operated Ca^{2+} channel Orai1 and its internalization during meiosis. J Cell Biol 191:523–535
53. Tang Y, Stephenson JL, Othmer HG (1996) Simplification and analysis of models of calcium dynamics based on IP_3-sensitive calcium channel kinetics. Biophys J 70:246–263
54. Pizzo P, Lissandron V, Capitanio P, Pozzan T (2011) Ca^{2+} signalling in the Golgi apparatus. Cell Calcium 50:184–192
55. Huotari J, Helenius A (2011) Endosome maturation. EMBO J 30:3481–3500
56. Gerasimenko JV, Tepikin AV, Petersen OH, Gerasimenko OV (1998) Calcium uptake via endocytosis with rapid release from acidifying endosomes. Curr Biol 8:1335–1338
57. Choi YO, Park JH, Song YS, Lee W, Moriyama Y, Choe H, Leem CH, Jang YJ (2007) Involvement of vesicular H^+-ATPase in insulin-stimulated glucose transport in 3T3-F442A adipocytes. Endocr J 54:733–743
58. Khan SZ, Longland CL, Michelangeli F (2000) The effects of phenothiazines and other calmodulin antagonists on the sarcoplasmic and endoplasmic reticulum Ca^{2+} pumps. Biochem Pharmacol 60:1797–1806